Available online at www.sciencedirect.com
SCIENCE DIRECT®
Journal of Computational Physics 213 (2006) 862–875
JOURNAL OF COMPUTATIONAL PHYSICS
www.elsevier.com/locate/jcp

A new conservative unsplit method for the solution of the Vlasov equation

N.V. Elkina [a,b], J. Büchner [b,*]

[a] M.V. Keldysh Institute for Applied Mathematics Miusskaya sq., 4 Moscow 125047, Russia
[b] Max-Planck-Institut für Sonnensystemforschung, Max-Planck-Str. 2, 37191 Katlenburg-Lindau, Germany

Received 12 April 2005; received in revised form 21 July 2005; accepted 6 September 2005
Available online 8 November 2005

Abstract

We have developed a new conservative method for solving the Vlasov equation without using any splitting technique. Our goal is to maintain the positivity of the distribution function and to avoid un-physical oscillations which might lead to numerical instabilities. Based on a finite volume conservative discretization of the conservative form of the Vlasov equation we implemented a highly accurate second-order upwind scheme. In order to avoid un-physical oscillations and their possible numerical instability we apply a flux-limiter in the second order. We validate our new Vlasov solver by considering standard cases of one-dimensional current-driven ion-acoustic instabilities solving a Vlasov–Ampère set of equations.

Keywords: Collisionless plasma; High-resolution monotone method; Upwind central scheme; Finite volume method; Ion-acoustic instability

1. Introduction

The investigation of resonant wave-particle interactions and of the resulting anomalous transport properties of collisionless plasmas requires a kinetic approach. Since binary collisions are negligible in collisionless plasmas resonant wave-particle interactions are well described by the Vlasov equation, a Boltzmann equation with a vanishing right hand side (r.h.s.). While linear and weakly (quasi-) linear analytical theories exist, nonlinear resonance phenomena have to be studied by means of numerical simulation techniques.

The most common approach to a numerical solution of the Vlasov equation is the particle-in-cell (PIC) technique. PIC solvers approximately describe the plasma dynamics by a limited number of macro-particles, pushed around in the self-consistent average electromagnetic fields. The fields are obtained by calculating charge density and currents on an Eulerian grid. The main advantage of the PIC method is their (Lagrangian) use of the characteristics of the hyperbolic PDE which are taken into account in form of the particle orbits. This makes PIC codes easily extendable to multi-dimensional applications. The main disadvantage of the

* Corresponding author. Tel.: +49 5556 979 295; fax: +49 5556 979 6 295.
E-mail address: buechner@mps.mpg.de (J. Büchner).

0021-9991/$ - see front matter
doi:10.1016/j.jcp.2005.09.023

PIC-approach is the numerical noise due to the limited number of particles considered. With their finite particle number PIC codes practically cannot represent the details of the phase space evolution. For the practically available number of particles it is almost impossible to simulate details of fine scale resonance effects. This makes the PIC method inadequate for the accurate analysis, e.g. of warm plasma instabilities. To describe wave-particle resonances accurately one needs both a very high resolution of the phase space as well as a low noise level comparable with the thermal plasma fluctuations.

An alternative way to investigate collisionless plasma phenomena is the direct integration of the partial differential Vlasov equation. In contrast to PIC codes direct Lagrangian solvers of the Vlasov equation have follow the deformation of the boundaries of phase space elements. In a Lagrangian Vlasov solver the distribution function $f(x,v,t)$ can be seen as the evolving density of an incompressible "phase fluid", which stays constant within small subdomains. They were called "water bags" giving such method its name [1]. Due to Liouville's theorem the volume of each phase space element (subdomain) stays unchanged with time. Hence, if one would be able to follow the motion of the boundaries of the "water bag" (phase space element) one could determine the evolution of the distribution function. This can be done by advancing a sufficiently large number of points along the "water bag" (subdomain) boundary. The boundary points evolve along the characteristics of the Vlasov equation like particle trajectories in PIC solvers, both due to the action of the same average, self-consistent electromagnetic fields. Unfortunately, because of the non-dissipative nature of the Vlasov-equation, the subdomain boundary will spread out in the phase space becoming more and more filamented. To maintain an accurate description of the subdomain deformation eventually more and more points along its boundary would have to be considered. As a result already the simplest one-dimensional in space and velocity space (1D1V) "water bag" Lagrangian method of solving the Vlasov equation is computationally very expensive. Lagrangian Vlasov solvers are practically inapplicable to higher dimensional problems.

More appropriate for practical purposes (and widely used) are semi-Lagrangian solvers of the Vlasov equation. Semi-Lagrangian methods utilize the Lagrangian solution of the Vlasov equation based on the conservation of the distribution function along the characteristics of the PDE. After each time step, however, they have to interpolate the new function values back to Eulerian (fixed) grid points at which the fields are calculated [2]. This makes at least multi-dimensional semi-Lagrangian solvers very expensive. However, after splitting the Vlasov equation into a spatial and velocity space part, the two parts can be solved sequentially as demonstrated first for a one-dimensional equation [3] and later for higher dimensions as well [4]. Time-splitting reduces the semi-Lagrangian solution of the Vlasov equation to the solution of one-dimensional scalar transport equations. This considerably increases the efficiency of the solution. The disadvantage of such fractional splitting is the loss of synchronous, symmetric advancing of the distribution function in real and velocity space.

Fully Eulerian grid methods do not have to interpolate [5]. Unfortunately, Eulerian methods suffer from numerical diffusion due to truncation errors arising when calculating derivatives. While finite difference methods as the method of McCormac [6] break down near discontinuities, where the differential form of conservation laws does not hold, the accuracy of Eulerian methods can be increased by applying conservative solvers as done for a splitting approach in [7] (using a positive and flux conservative method – PFC). In order to additionally maintain the synchronous advancement of fluxes to prepare a numerically accurate simulation of relativistic problems including kinetic instabilities in hot plasmas, we were looking for a stable numerical scheme which accurately solves the conservative Vlasov equation while strictly maintaining a positive value of the distribution function and came to the conclusion that this goal could be reached by means of an unsplit conservative finite volume discretization (FVM) method.

Here, in this paper, we present our utilization of an unsplit finite volume discretization based on the Vlasov equation in its conservative form. Dividing the phase space into subdomains (cells) we consider the evolution of each cell-averaged distribution function $\bar{f}_{i,j}$ with time. The distribution function values are modified at each time step by the in- and outflow through the cell boundaries. This allows a conservative numerical solution, since flows added to one cell are at the same time as subtracted from other, neighboring cells. This way the total particle number and other moments of the distribution function are conserved. The main problem is to determine an appropriate flux function that approximates the flows through the cell boundaries reasonably well. For this purpose we utilize a cell-centered upwind scheme, well known in the computational fluid dynamics (CFD). In contrast to a finite difference discretization, upwind schemes take into account the information

about the flow direction contained in the Vlasov equation. Using the characteristics of the hyperbolic Vlasov PDEs, they differentiate directly the flow direction. Following Godunov [8], this can be done by solving the Riemann problem at the boundary between adjacent cells. While Godunov originally considered only first-order upwind schemes, we utilized a second-order scheme. The extension to second-order accuracy requires the incorporation of derivatives not only in the normal direction (as in one-dimensional or splitting algorithms), but also to calculate mixed derivatives arising in the second order of the Taylor series expansion. To avoid unstable oscillations, which can arise in higher order schemes near steep gradients (in case of the Vlasov equation due to phase space filamentation), in computational fluid dynamics usually two types of high-resolution schemes are used: flux limited transport (FLT) and flux corrected transport (FCT) schemes [9,10]. Unsplit FCT schemes were applied to solve the Vlasov equation in [11]. In computational fluid dynamics unsplit FLT schemes were proposed in [12–14]. In the spirit of these schemes we suggest a new flux limited conservative method to solve the Vlasov equation. In any Eulerian-grid based scheme the information about subgrid structures (filaments) is usually lost due to smoothing which leads to numerical loss of information. We take care that our scheme increases the system's entropy as little as possible, close to the grid based minimum level. To achieve this for a finite number of grid points we locally enhance the resolution in critical phase-space regions by grid stretching.

In Section 2, we list the basic equation to be solved, in Section 3 we formulate both the integral and differential conservative forms of the Vlasov equation, which we intend to solve numerically. In Section 4 we present our unsplit finite volume discretization scheme. After discussing the optimum grid scaling in Section 5.1 we validate our method by solving the Vlasov equation for two typical 1D1V problems. We apply it in a code consisting of a set of Vlasov–Ampère equations for initial and boundary conditions triggering (Section 5.2) and spontaneously exciting an ion-acoustic plasma instability (Section 5.3).

2. Basic equations

We intend to solve the Vlasov equation, which in the usually considered advection form, can be written as

$$\frac{\partial f_\alpha}{\partial t}+\vec{v}\frac{\partial f_\alpha}{\partial r}+\frac{e_\alpha}{m_\alpha}\left(\vec{E}+\frac{1}{c}[\vec{v}\times\vec{B}]\right)\frac{\partial f_\alpha}{\partial \vec{v}}=0, \tag{1}$$

where $\alpha = \mathrm{i}, \mathrm{e}$ stands for ions and electrons, respectively. For a Vlasov code, the average electromagnetic fields have to be determined self-consistently by solving Maxwell's equations:

$$\frac{1}{c}\frac{\partial \vec{B}}{\partial t}=-\nabla\times\vec{E},\quad \frac{1}{c}\frac{\partial \vec{E}}{\partial t}=\nabla\times\vec{B}-\frac{4\pi}{c}\vec{j}, \tag{2}$$

$$\nabla\cdot\vec{E}=4\pi\rho,\quad \nabla\cdot\vec{B}=0, \tag{3}$$

where c is the speed of light. Charge density (ρ) as well as the current density ($\vec{j}$) are moments of distribution function, which can be calculated as

$$\rho(\vec{r},t)=\sum_\alpha e_\alpha\int f_\alpha \mathrm{d}\vec{v},\quad \vec{j}(\vec{r},t)=\sum_\alpha e_\alpha\int \vec{v} f_\alpha \mathrm{d}\vec{v}. \tag{4}$$

We apply the normalization:

$$t=t'\omega_{\mathrm{pe}}^{-1},\quad v=v'c,\quad r=r'\frac{c}{\omega_{\mathrm{pe}}},\quad \vec{E}=\vec{E}'\frac{m_{\mathrm{e}}c\omega_{\mathrm{pe}}}{e},\quad \vec{B}=\vec{B}'\frac{m_{\mathrm{e}}c\omega_{\mathrm{pe}}}{e}, \tag{5}$$

where $\omega_{\mathrm{pe}}=\sqrt{4\pi\bar{\rho}_{\mathrm{e}}|e|/m_{\mathrm{e}}}$ is the plasma frequency, with m_{e} being the electron mass, e the elementary charge and $\bar{\rho}_{\mathrm{e}}=\bar{\rho}_{\mathrm{i}}$ (quasi-neutrality condition). Omitting in the following the apostrophes, Eqs. (1)–(3) obey the normalized form

$$\frac{\partial f_\alpha}{\partial t}+\vec{v}\frac{\partial f_\alpha}{\partial \vec{r}}+\frac{1}{C_\alpha}(\vec{E}+[\vec{v}\times\vec{B}])\frac{\partial f_\alpha}{\partial \vec{v}}=0, \tag{6}$$

$$\frac{\partial \vec{B}}{\partial t}=-\nabla\times\vec{E}\quad \frac{\partial \vec{E}}{\partial t}=\nabla\times\vec{B}-\vec{J}, \tag{7}$$

$$\nabla\vec{E}=\rho,\quad \nabla\vec{B}=0, \tag{8}$$

where $C_e = -1$ and $C_i = M_i/m_e$ for electrons and ions, respectively, and $\vec{J}$ is the normalized current – in contrast to the j-index used for in Section 4.

3. Conservative Vlasov equation

Since our goal is the development of a conservative discretization scheme for a broad class of Vlasov problems, including relativistic, we have to start with the conservative form of the Vlasov equation. The latter directly follows from the conservation of the number of particles in a six-dimensional phase space volume Ω, which, in agreement with the Liouville theorem, can be expressed as (we omit the index α indicating different particle species)

$$N = \int_\Omega f(\vec{r},\vec{v},t)\,\mathrm{d}^3r\,\mathrm{d}^3v = \int_\Omega f(\vec{R},t)\,\mathrm{d}\Omega = \text{constant}, \tag{9}$$

where $\vec{R} = \{\vec{r},\vec{v}\}$ is the six-dimensional phase space vector.

The total differentiation of Eq. (9) over time reveals

$$\frac{\mathrm{d}N}{\mathrm{d}t} = \int_\Omega \left\{ \frac{\partial f(\vec{R},t)}{\partial t} + \frac{\partial f}{\partial \vec{R}} \cdot \frac{\mathrm{d}\vec{R}}{\mathrm{d}t} \right\} \mathrm{d}\Omega = \int_\Omega \left(\frac{\partial f}{\partial t} + \nabla f \vec{U} \right) \mathrm{d}\Omega = 0, \tag{10}$$

where ∇ is the six-dimensional phase-space derivative, defined as

$$\nabla = \{\nabla_{\vec{r}}, \nabla_{\vec{v}}\} = \left\{ \frac{\partial}{\partial \vec{r}}, \frac{\partial}{\partial \vec{v}} \right\} = \frac{\partial}{\partial \vec{R}} \tag{11}$$

and $\vec{U}$ is the six-dimensional phase space flow vector defined as the total time derivative of $\vec{R}$

$$\vec{U} = \{\vec{U}_{\vec{r}}, \vec{U}_{\vec{v}}\} = \frac{\mathrm{d}\vec{R}}{\mathrm{d}t} = \{\dot{\vec{r}}, \dot{\vec{v}}\} = \left\{ \vec{v}, \frac{\vec{F}}{m} \right\}. \tag{12}$$

For the second term in integrals (10) the Gauss theorem reveals

$$\int_\Omega \nabla f \vec{U}\,\mathrm{d}\Omega = \oint_{S(\Omega)} f(\vec{n}\cdot\vec{U})\,\mathrm{d}S, \tag{13}$$

where $S(\Omega)$ is the surface of the phase space volume and $\vec{n}$ its normal direction. Using expression (12), one obtains the integral form of the conservative Vlasov equation (10)

$$\frac{\partial N}{\partial t} = \frac{\partial}{\partial t}\int_\Omega f\,\mathrm{d}\Omega = \int_\Omega \frac{\partial f}{\partial t}\,\mathrm{d}\Omega = -\oint_{S(\Omega)} f(\vec{n}\cdot\vec{U})\,\mathrm{d}S, \tag{14}$$

Eq. (14) means that the rate of change of the number of particles inside a domain Ω equals the integral flux of f through the surface of the domain $S(\Omega)$.

Using expression (11) one obtains the local form of the conservative Vlasov equation

$$\frac{\partial f}{\partial t} + \nabla\cdot(f\vec{U}) = \frac{\partial f}{\partial t} + \frac{\partial}{\partial \vec{r}}(f\cdot\vec{v}) + \frac{\partial}{\partial \vec{v}}\left(f\frac{\vec{F}}{m} \right) = 0, \tag{15}$$

where $\vec{v}$ and $\vec{F}/m$ are dependent on $\vec{r}$ and $\vec{v}$, respectively, variables. Both the conservative form (15) and the usually used advection form of the Vlasov equation (6) are equivalent as one can find out by carrying out the partial differentiation in the conservative Vlasov equation (15) following the product rule

$$\frac{\partial f}{\partial t} + \vec{v}\cdot\frac{\partial}{\partial \vec{r}}f + \frac{\vec{F}}{m}\cdot\frac{\partial}{\partial \vec{v}}f + f\left\{ \frac{\partial}{\partial \vec{r}}\vec{v} + \frac{\partial}{\partial \vec{v}}\cdot\frac{\vec{F}}{m} \right\} = 0. \tag{16}$$

Since for the Vlasov equation the phase space element is incompressible (the Liouville theorem applies) $\partial\vec{v}/\partial\vec{r} + \partial(\vec{F}/m)/\partial\vec{v} = (\nabla \cdot \vec{U}) = 0$ from Eq. (16) follows that advection and conservative form of the Vlasov equation are equivalent.

In order to solve the Vlasov equation in its integral conservative form one also has to formulate suitable initial and boundary conditions. The r.h.s. of Eq. (14) means that the distribution function f flows with the phase space velocity $\vec{U}$ through the boundaries of a closed and connected domain Ω. Hence, the boundary $S(\Omega)$ can be split into an inflow and an outflow part (the no-flow boundary is considered separately) defined by:

- inflow: $\Gamma^- = \{\vec{r}, \vec{v} \in S | U_n < 0\}$;
- outflow: $\Gamma^+ = \{\vec{r}, \vec{v} \in S | U_n > 0\}$.

A Dirichlet boundary condition for the conservative Vlasov equation can, therefore, be given as

$$f_{t,\vec{r}} = g(t, \vec{R}) \quad \text{for } (t, \vec{R}) \in \Gamma(t), \tag{17}$$

where $\Gamma(t)$ is boundary of the phase space volume.

4. Finite volume discretization

In terms of the differential flux $\vec{H} = f \cdot \vec{U}$ the integral form of the Vlasov equation (14) writes

$$\frac{\partial}{\partial t}\int_{\Omega} f \, \mathrm{d}\Omega = -\oint_{S(\Omega)} \vec{H}\vec{n} \, \mathrm{d}S. \tag{18}$$

Let us demonstrate the idea of our finite volume unsplit discretization for a simple 1D1V case (x,v) with a rectangular boundary. We define the discretization control volumes (subdomains) introducing a rectangular grid in the (x,v) 1D1V phase space. This breaks the simulation domain Ω down into $N_x \times N_v$ non-overlapping subdomains (cells) $V_{i,j}$ such that

$$\Omega = \bigcup_{i,j=0}^{N_x \times N_v} V_{i,j}, \tag{19}$$

where N_x and N_v are the numbers of grid points in the x and v directions. Let us relate the distribution function $f_{i,j}$ to the center of a subdomain $V_{i,j}$ while the fluxes are defined as flowing through the subdomain boundaries as depicted in Fig. 1 (shown are the integral fluxes $G = \int_{t,\Delta S} H(f)\,\mathrm{d}S\,\mathrm{d}t$, see Eq. (24), instead of the differential fluxes H). The volume of a subdomain (cell) $V_{i,j}$ is given by $[\Delta x_i \times \Delta v_j] \times [t_n; t_{n+1}]$, where $\Delta x_i = x_{i+1/2} - x_{i-1/2}$ and $\Delta v_j = v_{j+1/2} - v_{j-1/2}$.

Let us introduce the averaged over the subdomain $V_{i,j}$ distribution function $f_{i,j}$ at t_n as

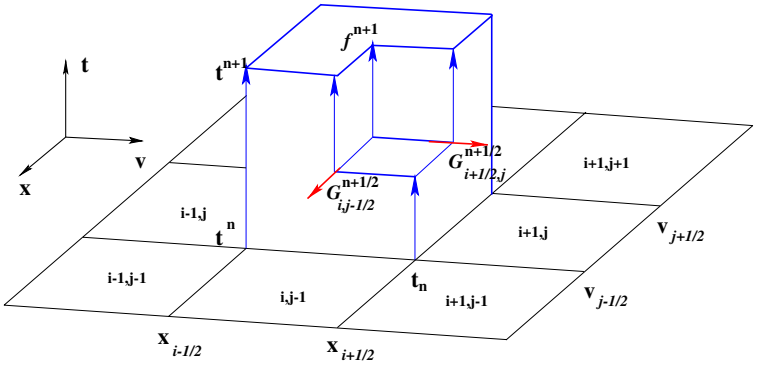

Fig. 1. Temporal–spatial subdomain structure of our FVD scheme.

$$\bar{f}^n_{i,j} = \frac{1}{|V_{i,j}|}\int_{V_{i,j}} f(\vec{r},\vec{v},t_n)\,\mathrm{d}V. \tag{20}$$

Then the integral conservative Vlasov equation in its form (18) can be expressed as

$$\frac{\partial \bar{f}^n_{i,j}}{\partial t} = -\frac{1}{|V_{ij}|}\int_{t_n}^{t_{n+1}}\oint_{\partial V_{ij}} \vec{H}_{i,j}\vec{n}_{i,j}\,\mathrm{d}S\,\mathrm{d}t, \tag{21}$$

where $\vec{n}_{i,j}$ denotes the outward directed normals of the subdomain (cell) boundary ∂V_{ij}. In our rectangular grid geometry each subdomain V_{ij} is bounded by four perpendicular sides $\Delta S_{i,j,\beta}$ (where $\beta = 1 \div 4$). Hence, the surface integral in (21) can be replaced by the sum over the fluxes through the four sides

$$\oint_{\partial V_{i,j}} \vec{H}(f)_{i,j}\vec{n}_{i,j}\,\mathrm{d}S = \sum_{\beta=1}^{4}\int_{\Delta S_{i,j,\beta}} \vec{H}(f)_{i,j}\vec{n}_{i,j,\beta}\,\mathrm{d}S. \tag{22}$$

Eqs. (21) and (22) establish a discrete evolution equation for the mean values of the distribution function $\bar{f}^n_{i,j}$. A finite volume method solves directly for the time advanced distribution function value. Hence, the discrete value of the distribution at t_{n+1} can be obtained as (in the following we omit the average-overline, i.e., $\bar{f}_{i,j} \to f_{i,j}$)

$$f^{n+1}_{i,j} = f^n_{i,j} - \frac{\Delta t}{|V_{i,j}|}\sum_{\beta=1}^{4} G^{n+\frac{1}{2}}_{i,j,\beta}. \tag{23}$$

In Eq. (23), we expressed the fluxes through the boundary segments $\Delta S_{i,j,\beta}$ by their discrete integral values $G^{n+1/2}_{i,j,\beta}$ which follow from Eqs. (21) and (22) as

$$G^{n+1/2}_{i,j,\beta} = \frac{1}{\Delta t}\int_{t_n}^{t_{n+1}}\int_{\Delta S} \vec{H}(f)\vec{n}_{i,j,\beta}\,\mathrm{d}S\,\mathrm{d}t. \tag{24}$$

In order to obtain a second-order accuracy time discretization we approximate the flux function at the center of each subdomain boundary at half the time step $(n+\frac{1}{2})$. Using the midpoint rule for the time integration one finds

$$G_{i,j,\beta=1,2} = \{G_{i\pm\frac{1}{2},j}\}, \quad G_{i,j,\beta=3,4} = \{G_{i,j\pm\frac{1}{2}}\}. \tag{25}$$

Each flux through a cell boundary depends on the cell to the left and on the cell to the right:

$$G_{i+\frac{1}{2},j,S} = g(G_{i+\frac{1}{2},j,L}, G_{i+\frac{1}{2},j,R}). \tag{26}$$

The determination of the flux through the subdomain (cell) boundaries $\delta V_{i,j}$ corresponds to the solution of a Riemann problem. At the beginning of each time step the fluxes set up an unsteady Riemann problem at each subdomain (cell) boundary. The solution of the Riemann problem determines the domain of dependence of each subdomain. Due to the causality principle one can approximate the solution at each time step inside the domain of dependence. For this purpose, we use the first-order Godunov flux functions [8]

$$G_{i+1/2,j} = U^+_x f_{i,j} + U^-_x f_{i+1,j}, \tag{27}$$

where

$$U^+_x = \max(U_x, 0), \quad U^-_x = \min(U_x, 0) \tag{28}$$

to obtain an upwind scheme. A numerical solution of the discrete conservative Vlasov equation (23), using first-order fluxes defined by Eqs. (27) and (28), would provide a first-order scheme with the stability condition [12]

$$\left|v\frac{\Delta t}{\Delta x}\right| + \left|\frac{F}{m}\frac{\Delta t}{\Delta v}\right| \leqq 1. \tag{29}$$

We enhance the accuracy of our scheme to the second order by introducing a more sophisticated approximation of the averaged quantities inside the subdomain using a piecewise-linear approximation based on a Taylor

series expansion of the subdomain boundary values for the determination of the fluxes inside the upwind cells. Let us describe the second-order approximation taking the calculation of $G_{i+\frac{1}{2},j}$ as an example (all other fluxes are calculated in the same way, just interchange the indices i, j and x, v). We define the left and right side flux function as: $G_{i+\frac{1}{2},j,S} \in (G_{i+\frac{1}{2},j,L}, G_{i+\frac{1}{2},j,R})$, where $G_{i+\frac{1}{2},j}$ is obtained by solving the Riemann problem

$$G_{i+\frac{1}{2},j} = g(G_{i+\frac{1}{2},j,R}, G_{i+\frac{1}{2},j,L}),$$

where

$$G^{n+\frac{1}{2}}_{i+\frac{1}{2},j,S} = U^+_x f^n_{i,j} + U^-_x f^n_{i+1,j} \pm \frac{\Delta x}{2}\frac{\partial f}{\partial x} + \frac{\Delta t}{2}\frac{\partial f}{\partial t}. \tag{30}$$

Substituting $\partial f/\partial t$ using the Vlasov equation (15) one obtains

$$G_{i,j,S} = U^+_x f^n_{i,j} + U^-_x f^n_{i+1,j} \pm \frac{\Delta x}{2}\frac{\partial f}{\partial x} + \frac{\Delta t}{2}\left(\frac{\partial H^x}{\partial x} + \frac{\partial H^v}{\partial v}\right) \tag{31}$$

and, after some rearrangement, one finds, the second-order upwind flux function

$$G_{i+1/2,j,S} = f_{i+k,j} + \left(\sigma_{i+1/2,j} - \frac{\Delta t}{\Delta x}U^x_{i+1/2,j}\right)H^x_{i+1/2,j} - \frac{\Delta t}{2}\frac{\partial H^v}{\partial v}, \tag{32}$$

where $\sigma_{i+1/2,j} = \mathrm{sign}(U^x_{i+\frac{1}{2},j})$. The first term in expression (32) provides a first-order upwind scheme. The middle term provides second-order accuracy correction. The third is a transverse propagation term from the diagonally located subdomain.

As it is well known second-order schemes can cause un-physical oscillations which may lead to negative values of the distribution function or even to numerical instabilities. To avoid such instabilities we limit the physical flux $H^x_{i+\frac{1}{2},j}$ in the middle, the second (order) term of Eq. (32). The limiter function, that applies directly to the derivatives, is given by

$$H^x_{i+1/2,j} = \mathrm{Limiter}\{Q^C_{i,j}, Q^R_{i,j}, Q^L_{i,j}\}, \tag{33}$$

where Limiter is a non-linear function based on the gradient of the solution. Near steep gradients the flux limitation reduces our method to a first-order upwind scheme. The central, right and left derivatives in the Limiter function (33) are given by

$$Q^C_{i,j} = f_{i+1,j} - f_{i-1,j}, \quad Q^R_{i,j} = f_{i+1,j} - f_{i,j}, \quad Q^L_{i,j} = f_{i,j} - f_{i-1,j}.$$

We successfully applied in our simulations the following flux limiter

$$\mathrm{Limiter}\{Q^C_{\mathrm{i}}, Q^R_{\mathrm{i}}, Q^L_{\mathrm{i}}\} = \begin{cases} \min\left\{\frac{1}{2}|Q^C_{i,j}|, 2|Q^L_{i,j}|, 2|Q^R_{i,j}|\right\}, & Q^R_{i,j}Q^L_{i,j} > 0. \\ 0, & \text{otherwise.} \end{cases} \tag{34}$$

A limiter in the form (34) satisfies the maximum principle, i.e., it does not introduce new extrema. This guarantees the absolute preservation of a positive (positivity) value of the distribution function.

Let us now consider the transverse propagation term in the expression for discrete integral flux function (32). We approximate it by choosing the Godunov function. If $H^{\mathrm{T}}_{i,j+1/2}$ is the solution of the Riemann problem projected along the v-direction with the left and right side expressions

$$(H^{\mathrm{T}}_{i,j+1/2,L}, H^{\mathrm{T}}_{i,j+\frac{1}{2},R}) = (U^v_{i,j+\frac{1}{2}} f^n_{i,j}, U^v_{i,j+\frac{1}{2}} f^n_{i,j+1}), \tag{35}$$

then the transversal term in Eq. (32) can be written as

$$\frac{\Delta t}{2}\frac{\partial H^v}{\partial v} = \frac{1}{2}\frac{\Delta t}{\Delta v}\left(H^{\mathrm{T}}_{v,i+k,j+\frac{1}{2}} - H^{\mathrm{T}}_{v,i+k,j-\frac{1}{2}}\right), \tag{36}$$

where $k = 0, \pm 1$ determine of the upwind subdomain.

Finally, after [12], the stability condition for the second-order scheme is given by

$$\max\left(\left|v\frac{\Delta t}{\Delta x}\right|,\left|\frac{F}{m}\frac{\Delta t}{\Delta v}\right|\right)\leqq 1. \tag{37}$$

5. Code validation of our new Vlasov solver

In order to validate our new Vlasov solver, we apply it to simulate the well known ion-acoustic (IA) plasma instability. For an electrostatic perturbation, the IA instability can be considered in one spatial (x) and one velocity space dimension ($v_x \to v$), i.e. in 1D1V. In the simplest case the instability causes just electrostatic oscillations in the x-direction ($E_x \to \langle E\rangle + E$). Hence, the Vlasov–Maxwell system of field equations (6)–(8) can be reduced to a set of two one-dimensional Vlasov and an one-dimensional Ampère equation for the perturbed current ($J_x \to \langle J\rangle + J$), to which an external current $J_{\text{ext}} = \langle J\rangle$ is added. This external, average current balances the average magnetic field ($\nabla \times \langle\vec{B}\rangle = \langle J\rangle = J_{\text{ext}}$) such that $\partial\langle E\rangle/\partial t = 0$ [6]

$$\frac{\partial f_\alpha}{\partial t} + v\frac{\partial f_\alpha}{\partial x} + \frac{1}{C_\alpha}\frac{\partial f_\alpha}{\partial v} = 0, \quad \frac{\partial E}{\partial t} = -J + J_{\text{ext}}. \tag{38}$$

To complete a code let us formulate a consistent with the Vlasov solver discretization of the electrostatic Ampère equation (38): Since the electric field enters the flux $G^{n+\frac{1}{2}}_{i,j\pm\frac{1}{2}}$ it is appropriate to determine E also at each half-time step $t^{n+1/2}$. Hence, $E_{i,j\pm 1/2}$ should be calculated as

$$E^{n+\frac{1}{2}}_{i,j\pm\frac{1}{2}} = E^{n-\frac{1}{2}}_{i,j\pm\frac{1}{2}} - \Delta t\cdot J^{n}_{i,j\pm\frac{1}{2}} \tag{39}$$

while the current $J^{n}_{i,j\pm\frac{1}{2}}$ should be calculated synchronously with the advancement of the distribution function.

5.1. Parameters of the space-time grid

First let us discuss the optimum choice of the grid sampling. The maximum possible time step size is determined by the stability condition (37). The corresponding necessary Courant–Friedrich–Levy (CFL) condition is CFL $\leqslant 1$.

We choose the time step Δt determined in the (1D1V) phase space for both electrons and ions plasma species in whole simulation domain in accordance with

$$\Delta t = \text{CFL}\cdot\min\left[\frac{\Delta x}{\max(v^{\text{e}}_{\max}, v^{i}_{\max})}, |C_{\text{e}}|\cdot\left(\frac{\Delta v^{\text{e}}}{E^{\max}_x}\right), |C_{\text{i}}|\cdot\left(\frac{\Delta v^{i}}{E^{\max}_x}\right)\right], \tag{40}$$

where $v^{\max}_{\text{e}}$ and $v^{\max}_{\text{i}}$ are the maximum velocities in the simulation box for the plasma species and $E^{\max}_x$ is the maximum electric field. CFL $= 0.8$ is used for all simulation runs presented here.

The necessary condition for grid sampling in the real space is the of quasi-neutrality condition, which requires a resolution of the Debye length $\lambda_{\text{D}} = v_{\text{te}}/\omega_{\text{pe}}$, where $v_{\text{te}} = \sqrt{T_{\text{e}}/m_{\text{e}}}$ and T_{e} is the electron temperature in energy units

$$\Delta x < \lambda_{\text{D}}. \tag{41}$$

The choice of the number of spatial and velocity space Eulerian grid points for the numerical integration of the discrete solution determines the smallest phase space filaments, which can be resolved. The choice of Δv determines, therefore, the smoothing, i.e., the minimum numerical dissipation in the system. The concrete choice of the velocity space resolution, always depends on the problem studied. Δv_{i}, for example, should be much smaller than any physically relevant velocity space granulation.

Let us investigate the influence of the grid scales on the dissipative properties of our scheme. While the Vlasov equation itself is non-dissipative (Hamiltonian), (numerical) dissipation arises due to its discrete representation on an Eulerian grid. Once the forming microstructures (filaments) reach the mesh-size scale, any finer filamentation becomes smoothed away numerically. At the same time, large scale structures are unaffected. The evolution on these fine scales can be estimated from the solution of the free-streaming Vlasov equation, Fourier transformed in the real space ($f(v,x,t) \to f(v,k,t)$)

$$f(v,k,t) = f(v,k,0)\mathrm{e}^{\mathrm{i}\eta v}. \tag{42}$$

When $\eta = kt$ reaches the inverse of Δv one cannot any more follow the further filamentation of f, the information about which is lost. This takes place especially within $\Delta = \eta^{-1} = 1/kt$ of the resonance velocity, i.e., Δ is the characteristic width of the resonance. Only particles within Δ of the resonance velocity experience a significant contribution to or deduction of its kinetic energy [15]. The linear stage ends at saturation. Single-mode systems saturate when the electric field reaches an amplitude E_{sat} for which the trapping frequency is of the order of the linear growth rate γ of a given instability

$$\omega_t = \sqrt{\frac{eE_{\mathrm{sat}}k}{m_{\mathrm{e}}}} \simeq \gamma,$$

which can be derived solving the linear dispersion relation. The characteristic saturation time may be estimated for an initial perturbation δE_0, since $E_{\mathrm{sat}} = \delta E_0 \mathrm{e}^{\gamma t_{\mathrm{sat}}}$, as

$$t_{\mathrm{sat}} = \frac{1}{\gamma}\ln\left(\frac{\gamma^2 m}{e\delta E_0}\right).$$

Thus, the characteristic width of the resonance region at saturation may be estimated as

$$\Delta = \frac{1}{kt_{\mathrm{sat}}} = \frac{\gamma}{k\ln(\gamma^2 m/e\delta E_0)}, \tag{43}$$

which should be resolved by the velocity space grid

$$\Delta v \ll \Delta. \tag{44}$$

A way to decrease the numerical dissipation without increasing the total number of grid cells is the use of a non-uniform grid stretching which refined the mesh at places where the finest filaments are expected, i.e., near resonances, while stretching it away from the resonances. This can be done when the main resonance region is known. In our example this is the ion-acoustic wave velocity, the ion-sound speed $c_{\mathrm{ia}} = \sqrt{T_{\mathrm{e}}/M_{\mathrm{i}}}$. Consequently, we applied a stretching function

$$V_{\mathrm{i}}^{\mathrm{str}} = v^{\max}\frac{\sinh((v_{\mathrm{i}} - v_{\mathrm{res}})\mathrm{Str}/v^{\max})}{\sinh(\mathrm{Str})}, \tag{45}$$

where Str is the stretching factor, $V_{\mathrm{i}}^{\mathrm{str}}$ is the velocity value on the non-uniform grid and v_{i} the velocity value on the original, equally spaced grid, $v_{\mathrm{res}} = c_{\mathrm{ia}}$ and $v^{\max}$ is the maximum velocity considered. We perform simulations with the non-equidistant distribution of velocity space grid points $V_{\mathrm{i}}^{\mathrm{str}}$ which concentrate near the resonance velocity for simulation of the ion-acoustic turbulence (see Section 5.2). Fig. 2 depicts the electron distribution function at an instantaneous moment of time on the non-uniformly stretched near the resonance velocity space grid surface.

5.2. Triggered ion-acoustic instability

In order to physically validate our Vlasov solver we choose the problem of onset and saturation of an IA instability in a system with an electron distribution function drifting against a background of a resting ion distribution. We first modulated the electron distribution in space in order to trigger a whole spectrum of unstable waves (this section), while we will discuss the results of a simulation of a spontaneous IA instability in the following section.

In order to trigger a multimode IA instability we use electron and ion distribution functions given by:

$$\begin{aligned} f_{\mathrm{e}} &= (1 + a^{\mathrm{e}}(x))\sqrt{\frac{1}{\pi\cdot v_{\mathrm{te}}^2}}\exp\left(-\frac{(v_{\mathrm{e}} - v_{\mathrm{de}})^2}{2v_{\mathrm{te}}^2}\right), \\ f_{\mathrm{i}} &= \sqrt{\frac{1}{\pi\cdot v_{\mathrm{ti}}^2}}\exp\left(-\frac{v_{\mathrm{i}}^2}{2v_{\mathrm{ti}}^2}\right), \end{aligned} \tag{46}$$

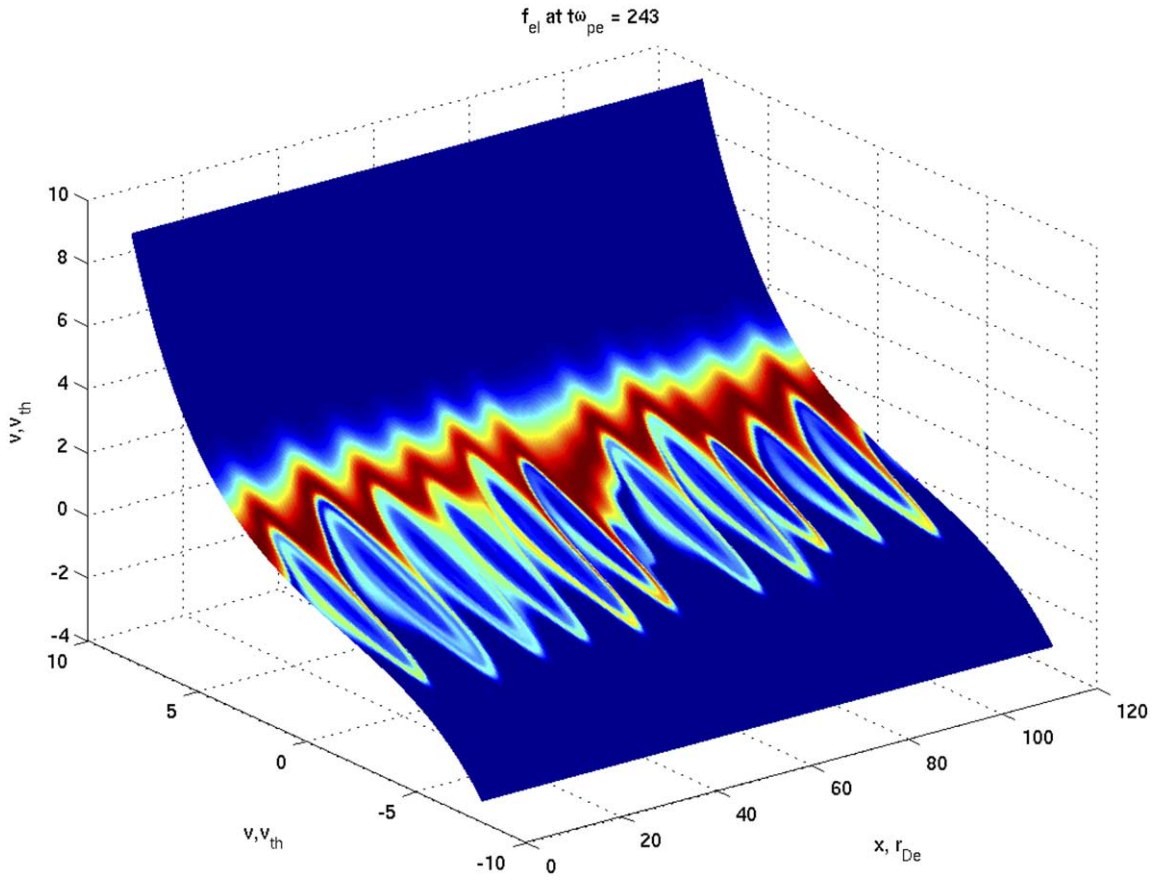

Fig. 2. Filamented electron phase space obtained with Str = 2 on a stretched 512×512 grid (for a triggered ion-acoustic instability – see Section 5.2).

where $v_{t\alpha} = \sqrt{T_\alpha/m_\alpha}$ (T_α is the temperature) are the electron and ion thermal velocities, respectively, and v_{de} is the drift speed of the electrons as suggested by Arber and Vann [5]. We used for the perturbation of the initial electron distribution function $a^e(x)$ the form function

$$a^e(x) = 0.01(\sin(x) + \sin(0.5x) + \sin(0.15x) + \sin(0.2x) + \cos(0.25x) + \cos(0.3x) + \cos(0.35x)). \quad (47)$$

Notice that, both distribution functions (46) are divided by the total number of particles (N_α), i.e.,

$$\int_{-\infty}^{\infty} f_\alpha \, dv_\alpha = 1. \quad (48)$$

Let us discuss the results of runs carried out for the following physical parameters:

$$C_i = M_i/m_e = 1000; \quad T_i = 0.5T_e; \quad T_e = 10 \text{ eV}; \quad v_{de} = 2v_{te}. \quad (49)$$

The parameters of the numerical scheme were

$$L_x = 0.1\frac{c}{\omega_{pe}} \approx 120\lambda_D; \quad v_e^{max} = 8v_{te}, \quad v_i^{max} = 8v_{ti}. \quad (50)$$

We used periodic boundary conditions in the real space. In the velocity space dimension we used Dirichlet boundary condition (17) with constant value f on the velocity space boundary, determined by initial condition.

For a run with $N_x = 512 \times N_v = 512$, the resulting evolution of the electron distribution, spatially averaged over the box L_x, is shown in Fig. 3. For the physical parameters given by Eq. (49) ion-acoustic waves start to grow. As can see in Fig. 3 considerable deformation of the drifting electron distribution space averaged

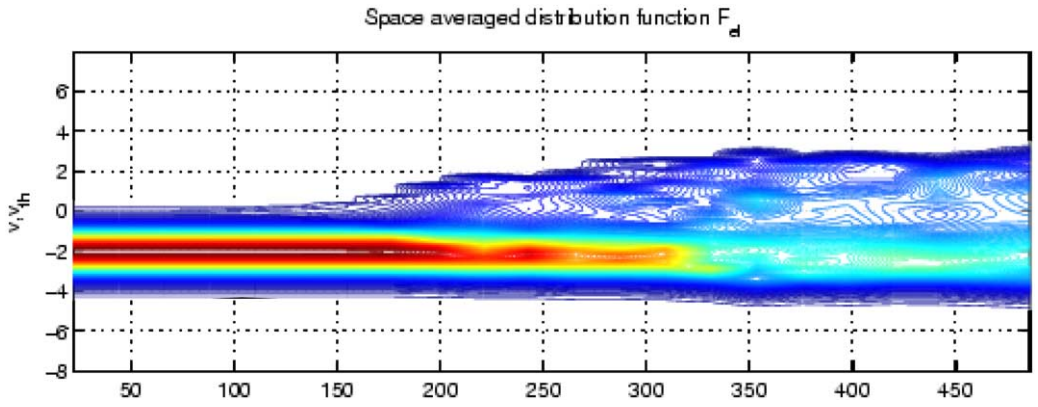

Fig. 3. Time evolution of the spatially averaged electron distribution function $f_e = F_e$ in the course of an ion-acoustic instability, $N_x \times N_v = 512 \times 512$.

function begins at about $t\omega_{pe} = 150$. The reason is that the growing ion sound waves obtain energy from the drifting electron distribution and transfer energy to the ions via resonant interaction of the fluctuating electric field with the particles. This leads to a deformation of the distribution functions of the electrons as shown in Fig. 3, finally causing a transition from quasi-linear to strongly non-linear wave particle interactions after about $t\omega_{pe} = 200$.

The loss of information, which characterizes the numerical diffusivity of the code, can be quantified by means of the relative distribution function entropy

$$S_{rel} = [S(t) - S(0)]/S(0), \text{ where } S(t) = -\int f \ln f \, dv \, dx. \tag{51}$$

Eq. (51) determines S_{rel} in a way that it stays zero for a strictly Hamiltonian, non-dissipative system ($S(t) = \text{constant}$), while it will monotonically grow for any discrete Eulerian grid based numerical scheme. Therefore, the value of S_{rel} quantifies the deviation from the ideal dissipationless state.

Let us compare the growth of S_{rel} for simulation runs with different choices of a fixed Eulerian grids: *Run* 1: $N_v \times N_x = 128 \times 256$, *Run* 2: $N_v \times N_x = 256 \times 256$, *Run* 3: $N_v \times N_x = 512 \times 512$. The relative entropy evolution in the course of these runs is depicted in Fig. 4. As one can see the numerical entropy is of the order of a few % even for the most coarse grid $N_v \times N_x = 128 \times 256$. S_{rel} decreases to even smaller values for finer fixed grids. Fig. 4 depicts also the relative entropy for the stretched grid case (Str = 2) with $N_v \times N_x = 512 \times 512$ grid points. Due to the stretching Str = 2 becomes much smaller in the linear and quasi-linear growth phase of the instability, if compared to the run with the same number but equidistant grid points.

5.3. Spontaneous ion-acoustic instability

For further physical validation of our new conservative scheme we choose to simulate also a spontaneously arising IA instability in a current carrying plasma. A spontaneous ion-acoustic instability is excited only if $v_{de} > v_{crit}$. The value of v_{crit} can be determined by solving the linear dispersion relation. Instead of imposing an electron drift as in the case of the ion-acoustic instability considered in Section 5.2, we apply a constant electric field to an initially unperturbed system of Maxwellian distributed electrons and ions. Since a Vlasov code is noiseless we have to add fluctuations δf_α to the distribution function as well

$$f_\alpha = \sqrt{\frac{1}{\pi \cdot v_{t\alpha}^2}} \exp\left(-\frac{(v_\alpha)^2}{v_{t\alpha}^2}\right) \cdot \left(1 + \frac{\delta f_\alpha}{f_\alpha}\right). \tag{52}$$

In our simulations, we have chosen a fluctuation amplitude at the thermal noise level. Initially, both electrons and ions are accelerated in an external electric field E_0^{ext}. When their relative drift reaches the critical speed v_{crit}, the plasma becomes unstable and ion-acoustic waves are generated. Omura et al. [16] investigated this problem

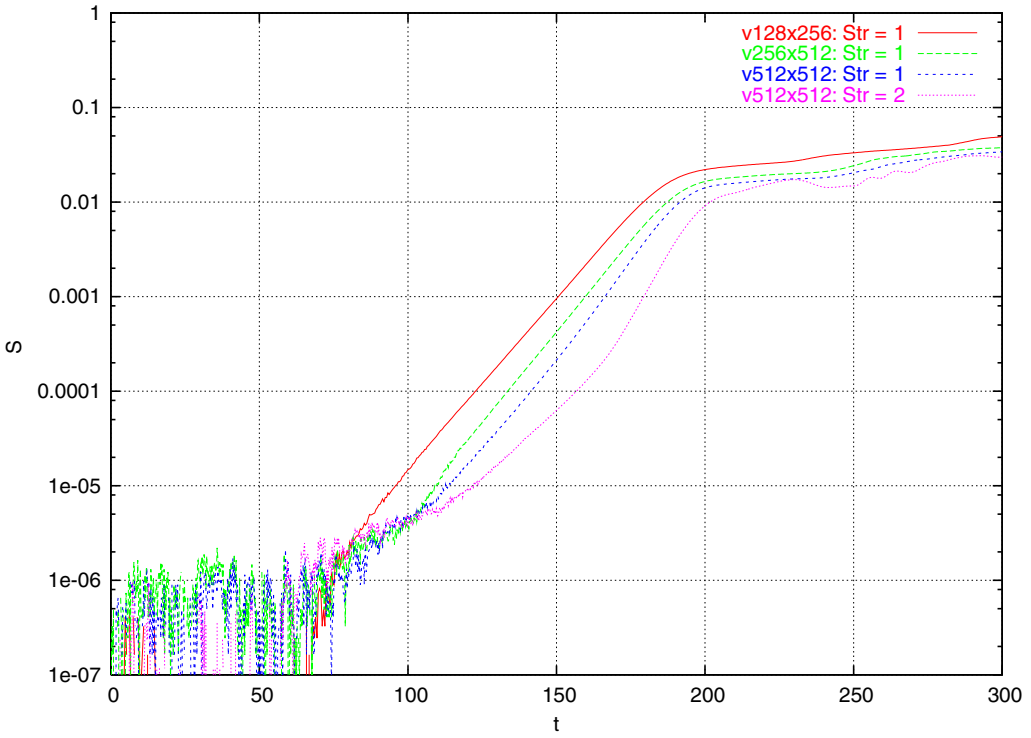

Fig. 4. Relative entropy evolution in the ion-acoustic instability simulation for high-resolution fixed grids and a lower overall resolution stretched grid.

by means of their one-dimensional PIC code KEMPO1. For better comparison of the results, we use the same ratio of ion to electron thermal velocities and apply the same external electric field strength

$$v_{\mathrm{ti}} = 0.0625 v_{\mathrm{te}}; \quad E_0^{\mathrm{ext}} = 0.01.$$

The other simulation parameters were

$$C_{\mathrm{i}} = M_{\mathrm{i}}/m_{\mathrm{e}} = 100; \quad T_{\mathrm{i}} = 0.4 T_{\mathrm{e}}; \quad T_{\mathrm{e}} = 10\ \mathrm{eV}$$

while the parameters of the numerical scheme were

$$L_x = c/\omega_{\mathrm{pe}} \approx 460 \lambda_{\mathrm{D}}, \quad v_{\mathrm{e}}^{\max} = 12 v_{\mathrm{te}}, \quad v_{\mathrm{i}}^{\max} = 12 v_{\mathrm{ti}}.$$

The grid resolution of the simulation was $N_x \times N_v = 256 \times 256$.

As one can see in the upper panel of Fig. 5, after about $t\omega_{\mathrm{pe}} = 400$ electric field fluctuations start to grow strongly The lower panel of Fig. 5 shows that the instability starts as soon as the drift velocity reaches $v_{\mathrm{crit}} = 2.3 v_{\mathrm{te}}$. After $t\omega_{\mathrm{pe}} = 400$ and until $t\omega_{\mathrm{pe}} = 500$, the strongly non-linear wave-particle resonant interaction reduces the drift speed (Fig. 5, lower panel). Then the resonance condition is not fulfilled any more and the electric field fluctuation energy decreases again, which allows the drift to grow further. Fig. 6 depicts the evolution of the spatially averaged electron distribution showing the quasi- and non-linear formation of a plateau in the electron distribution function. Our simulation results clearly indicate the long term stability of the new unsplit conservative Vlasov solver, described in Section 4.

6. Summary and outlook

The usually used splitting schemes practically usually solve the Vlasov equations in its advection form, where velocity and acceleration are considered as independent variables. Instead we have developed a conservative unsplit numerical method solving the Vlasov equation in its conservative form. Our flux limiting finite

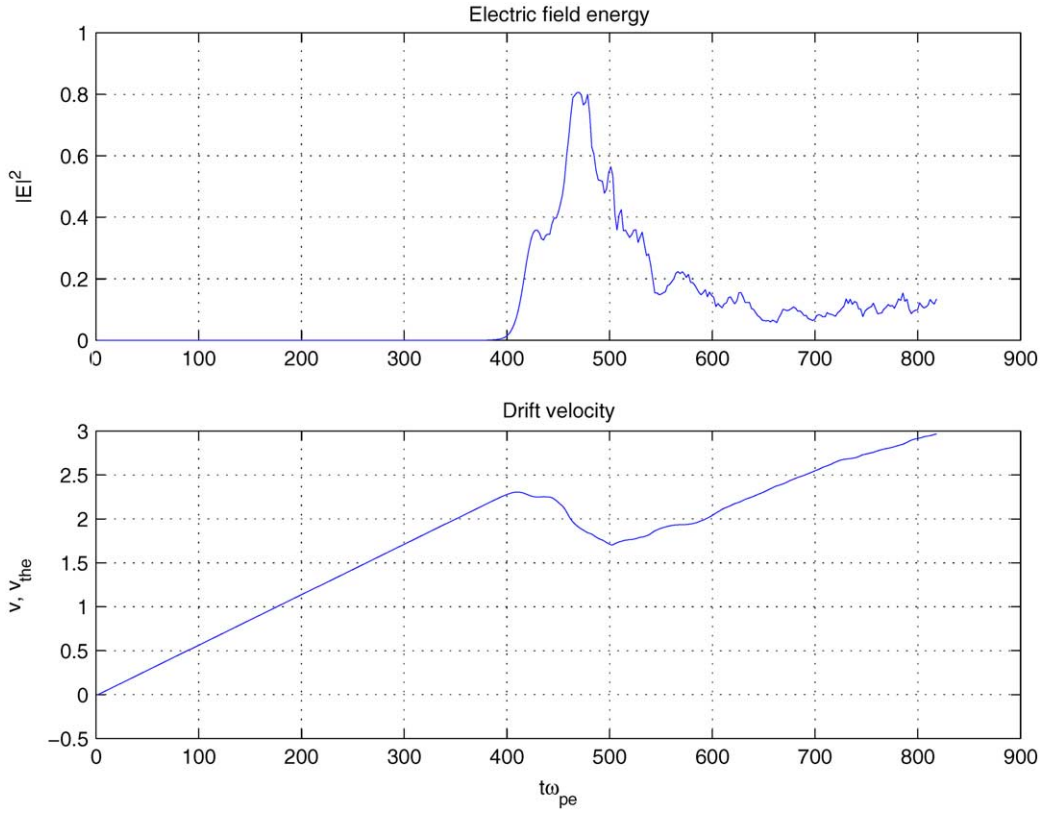

Fig. 5. Time evolution of the energy of the electric field fluctuations (upper panel) and of the average particle drift (current) velocity.

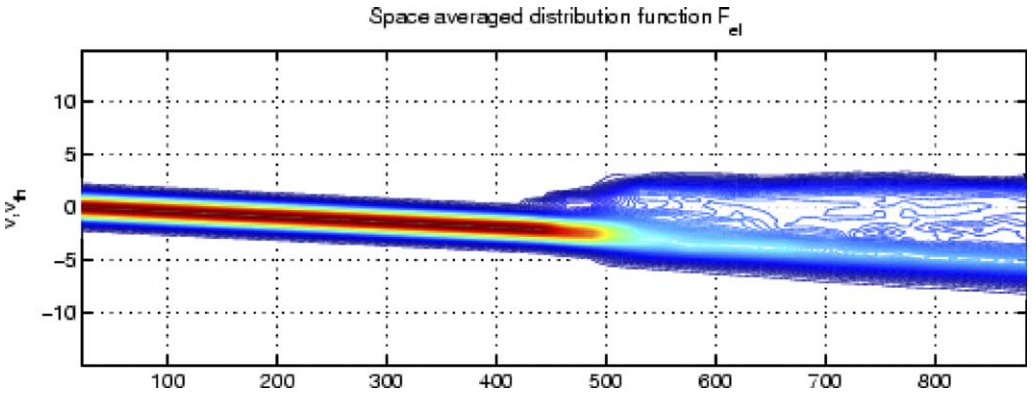

Fig. 6. Evolution of the spatially averaged electron distribution function $f_e = F_e$ in the course of the development of a spontaneous ion-acoustic instability, $N_x \times N_v = 256 \times 256$.

volume method maintains the positivity of the distribution function and guarantees the conservation of its moments, high accuracy, efficiency and performance. Physically we validated our new method by applying it to 1D1V simulations of both a triggered and a spontaneously excited ion-acoustic instability. For this sake, we developed a Vlasov–Ampère code based on our new Vlasov solver. We have studied the growth of the entropy of the solution caused by numerical truncation errors. We found that the entropy stays small even in the highly non-linear stage of a multi-mode triggered ion-acoustic instability. We also showed how the entropy can easily be further lowered by phase space grid stretching.

Our conservative unsplit method can be generalized to higher dimensions as well as to the solution of the relativistic Vlasov-equations in its conservative form. By applying a conservative Vlasov solver based on the principles presented here in this paper it might be possible to overcome the difficulties arising in the simulation of relativistic plasma instabilities [17].

References

[1] F.H. Hohl, M. Feix, Numerical experiments with a one-dimensional model for a self-gravitating star system, Astrophys. J. 147 (1964) 1164.
[2] A. Ghizzo, F. Huot, P. Bertrand, A non-periodic 2D semi-Lagrangian vlasov code for laser-plasma interaction on parallel computer, J. Comput. Phys. 186 (2003) 47–69.
[3] C. Cheng, G. Knorr, The integration of the Vlasov equation in configuration space, J. Comput. Phys. 22 (1976) 330–351.
[4] A. Mangeney, F. Califano, C. Cavazzoni, P. Travnicek, A numerical scheme for the integration of the Vlasov–Maxwell system of equations, J. Comput. Phys. 179 (2002) 495–538.
[5] T. Arber, R. Vann, A critical comparison of Eulerian-grid-based Vlasov solvers, J. Comput. Phys. 180 (2001) 339–357.
[6] R. Horne, M. Freeman, A new code for electrostatic simulation by numerical integration of the Vlasov and Ampère equations using MacCormack's method, J. Comput. Phys. 171 (2001) 182–200.
[7] F. Filbet, E. Sonnendrucker, P. Bertrand, Conservative numerical schemes for the Vlasov equation, J. Comput. Phys. 172 (2001) 166–187.
[8] S.K. Godunov, Finite difference method for the computation of discontinuous solutions of the equations of fluid dynamics, Mat. Sb. 7 (1959) 271–306.
[9] J.P. Boris, D. Book, Flux-Corrected Transport I. SHASTA, a fluid transport algorithm that works, J. Comput. Phys. 11 (1973) 38–69.
[10] S.T. Zalesak, Fully multidimensional Flux-Corrected Transport algorithms for fluids, J. Comput. Phys. 31 (1979) 335–362.
[11] J. Boris, D. Book, Solution of continuity equations by the method of Flux-Corrected Transport, Adv. Res. Appl. 16 (1985) 85–128.
[12] P. Colella, Multidimensional upwind methods for hyperbolic conservation law, J. Comput. Phys. 87 (1991) 171–200.
[13] J. Saltzman, An unsplit 3D upwind method for hyperbolic conservation laws, J. Comput. Phys. 115 (1994) 153–168.
[14] J.O. Langseth, R.J. LeVeque, A wave propagation method for three-dimensional hyperbolic conservation laws, J. Comput. Phys. 165 (2000) 126–166.
[15] T. O'Neil, Collisionless damping of nonlinear plasma oscillations, Phys. Fluid 8 (12) (1965) 2255–2262.
[16] Y. Omura, W. Heikkila, T. Umeda, K. Ninomiya, H. Matsumoto, Particle simulation of response to an applied electric field parallel to magnetic field lines, JGR 108 (A5) (2003) 1197.
[17] F. Huot, A. Ghizzo, P. Bertrand, E. Sonnendücker, O. Coulaud, Instability of the time splitting scheme for the one-dimensional and relativistic Vlasov–Maxwell system, J. Comput. Phys. 185 (2003) 512–531.